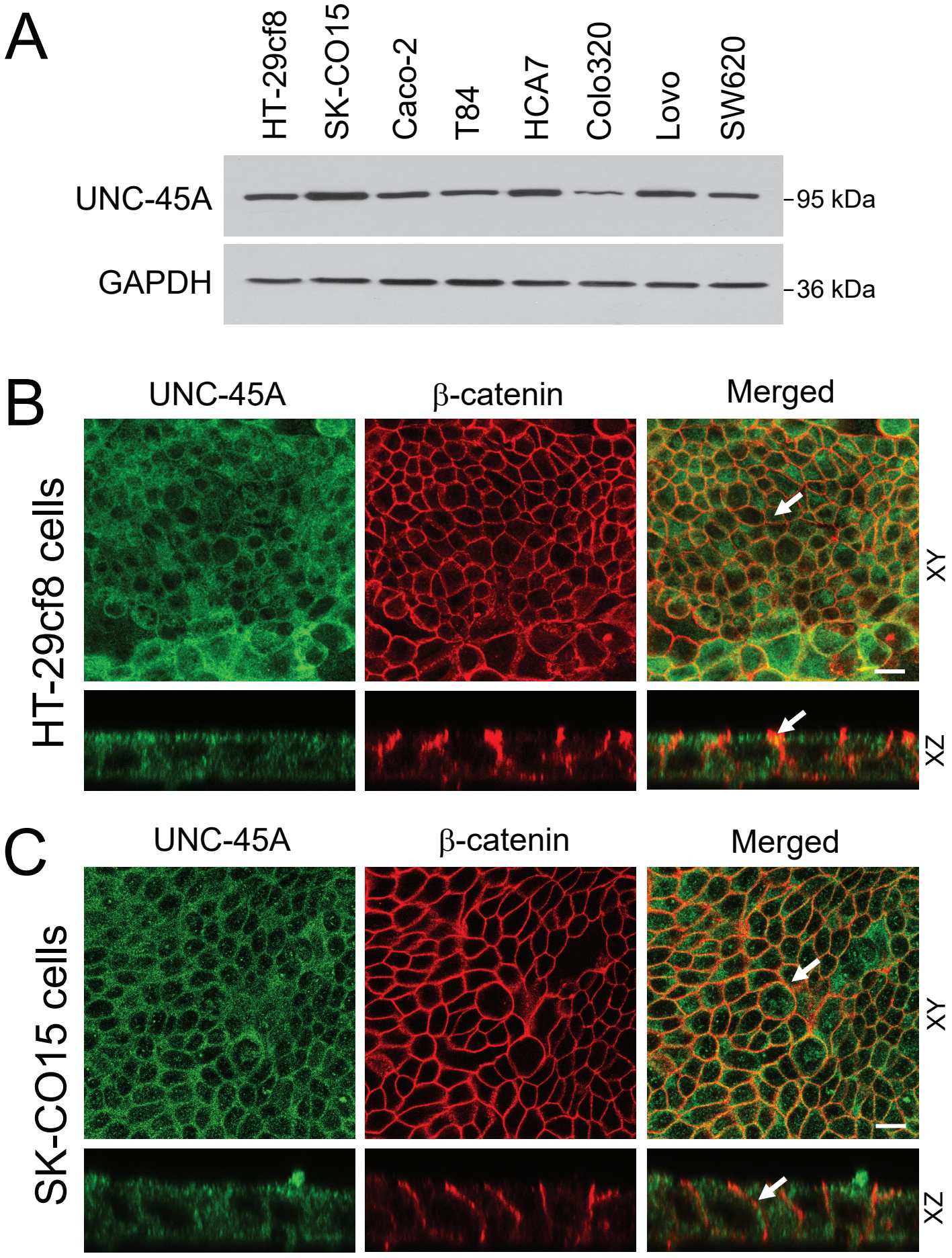

Figure S1. Expression and localization of UNC-45A in polarized model intestinal epithelial cell monolayers. (A) Immunoblotting analysis of UNC-45A expression in a panel of different human intestinal epithelial cell lines. (B,C) Dual immunofluorescence labeling of UNC-45A (green) and β-catenin (red) in polarized HT-29cf8 (B) and SK-CO15 (C) cell monolayers. Representative microscopic images of apical (xy) and lateral (xz) sections are shown. Arrows indicate enrichment of UNC-45A at apical junctions. Scale bars, 20 μm. A and B/C data are representative of two and three independent experiments, respectively.

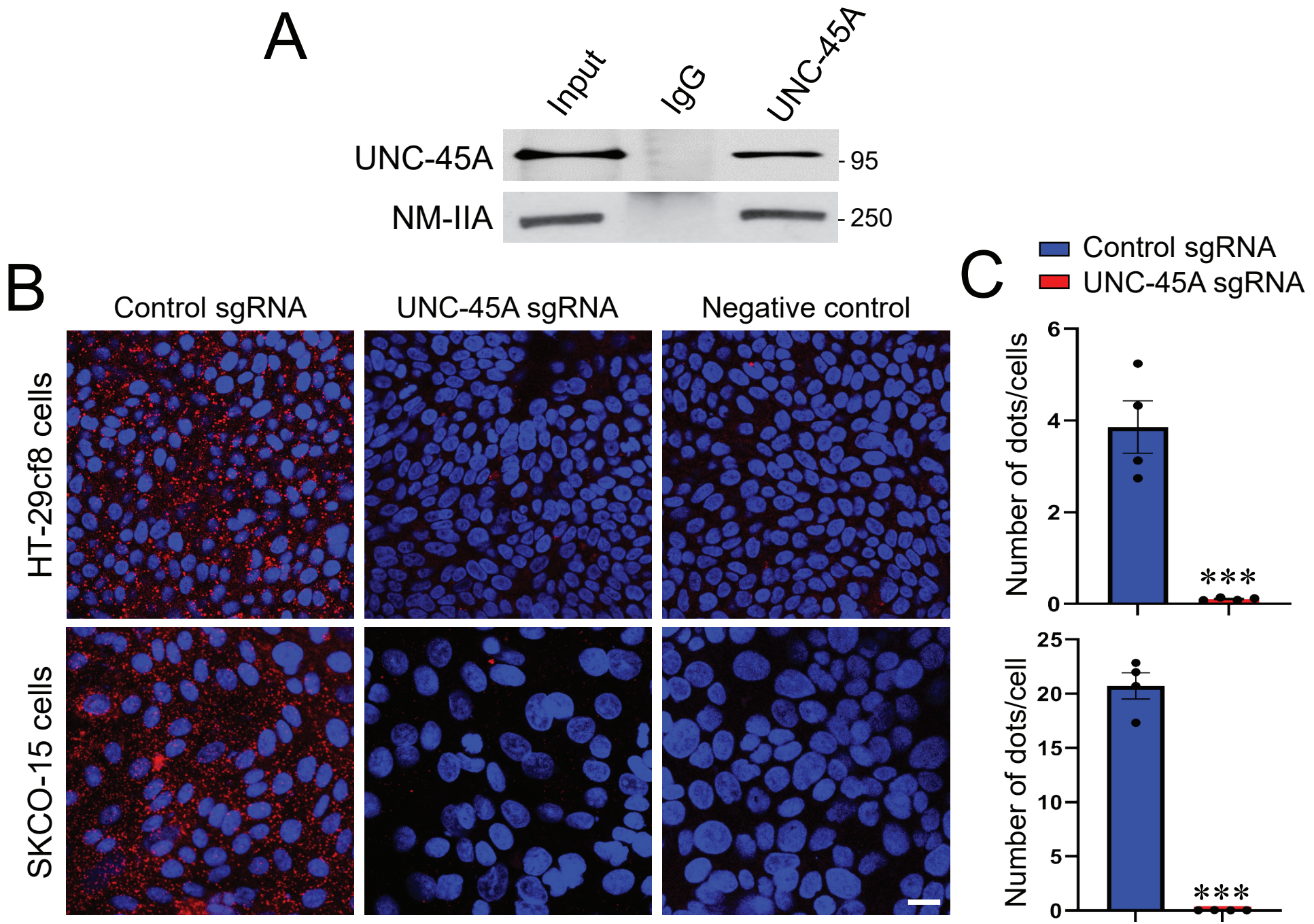

Figure S2. UNC-45A interacts with NM-IIA in polarized intestinal epithelial cell monolayers. (A) Immunoprecipitation analysis of UNC-45A-NM-II interactions in SK-CO15 cells. UNC-45A was pulled-down with anti-UNC-45A antibody. A pull-down with rabbit IgG served as a control. Immunoprecipitates were probed for UNC-45A and NM-IIA. (B,C) Proximity ligation assay using a pair of UNC-45A and NM-IIA antibodies in control and UNC-45A-depleted IEC. Representative fluorescence microscopy images (B) and quantification of the number of dots indicating interactions (C) are shown. For the negative control, the NM-IIA antibody was omitted. Means ± SE (n=4); ***P< 0.0005. Scale bar, 20 μm. A-C data are representative of two independent experiments.

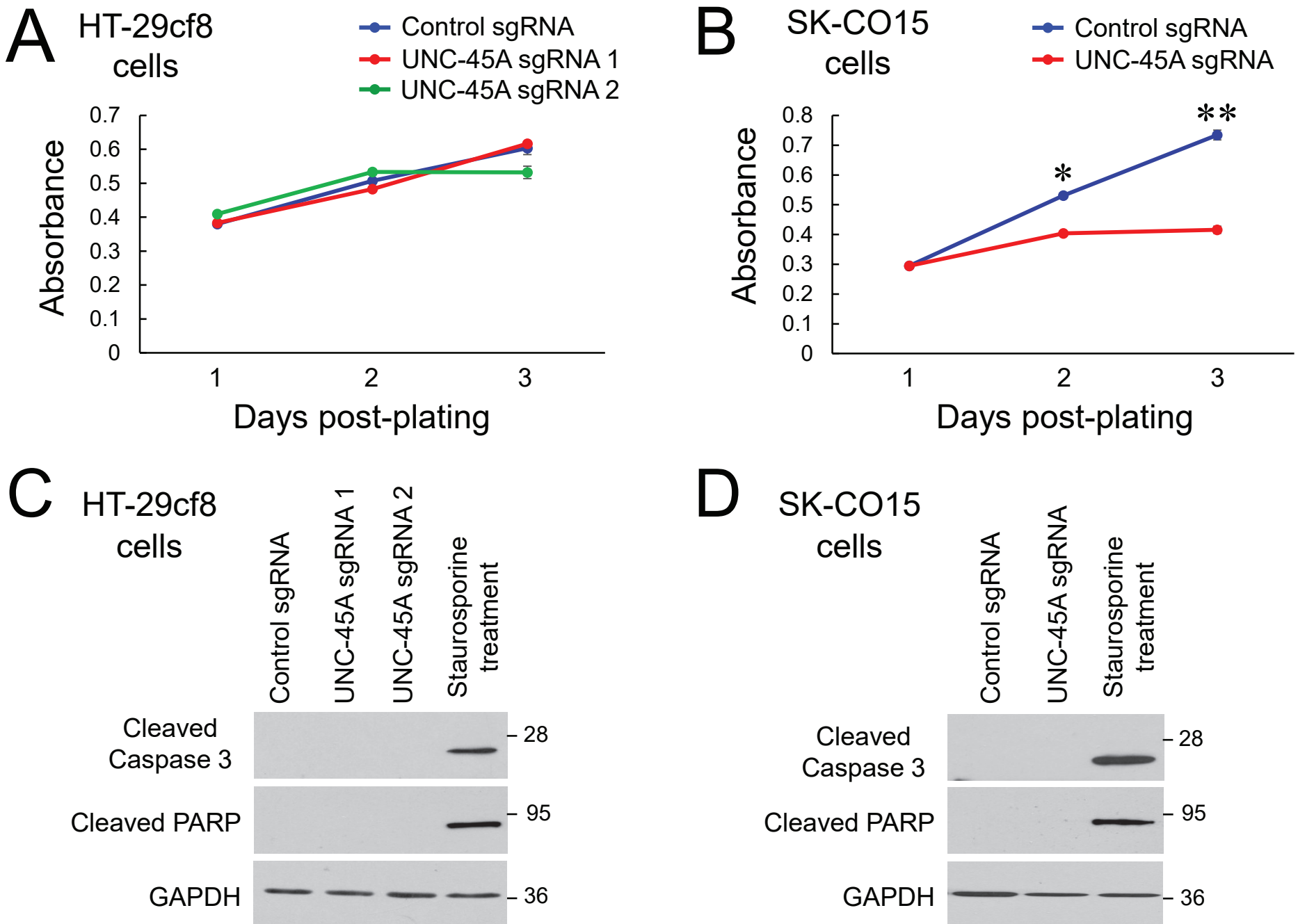

Figure S3. Loss of UNC-45A attenuates proliferation of SK-CO15, but not HT-29 cells without causing cell apoptosis. (A,B) MTT assay of control and UNC-45A-depleted HT-29cf8 (A) and SK-CO15 (B) cells at different times post-plating. Means ± SE (n=3); *P< 0.05, **P< 0.01. (C,D) Immunoblotting analysis of cleaved caspase 3 and cleaved PARP in total cell lysates of control and UNC-45A-depleted HT-29cf8 (C) and SK-CO15 (D) cells. Staurosporine treatment was used as a positive control for apoptosis induction. A-D data are representative of three independent experiments.

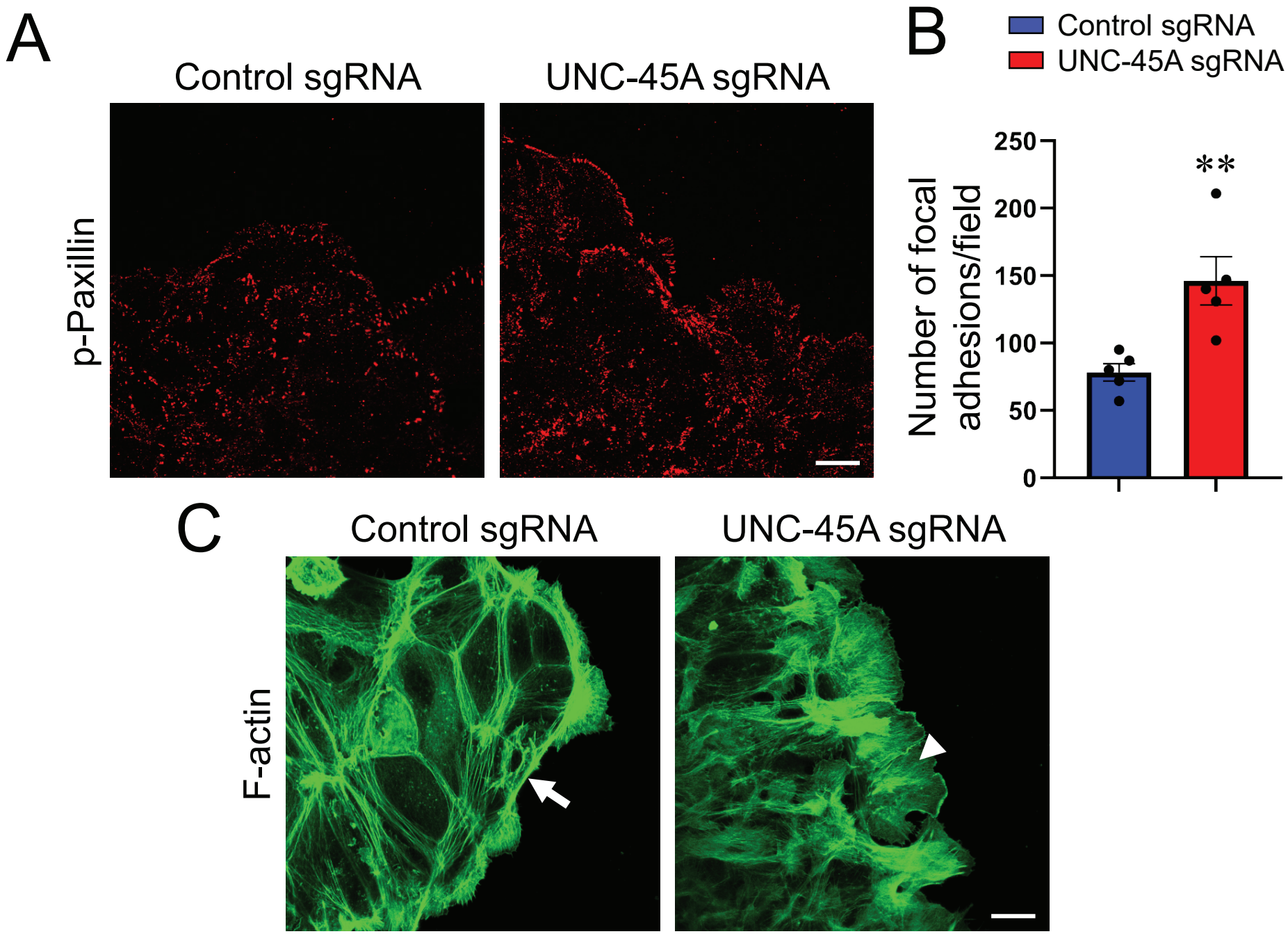

Figure S4. UNC-45A regulates assembly of focal adhesions and organization of the actin cytoskeleton in migrating intestinal epithelial cells. (A,B) Immunofluorescence labeling of a focal adhesion marker, phosphorylated (p) paxillin, at the leading edge of wounded control and UNC-45A-depleted SK-CO15 cell monolayers. Representative confocal microscopy images (A) and quantification of the focal adhesion number (B) are shown. Each dot represents the average number of focal adhesion counted in three different images. Means ± SE (n=4); **P< 0.005. Scale bar 20 μm. (C) Confocal microscopy images of F-actin labeling at the leading edge of migrating control and UNC-45A-depleted SK-CO15 cell monolayers. Scale bar, 20 μm. A-C data are representative of three independent experiments.

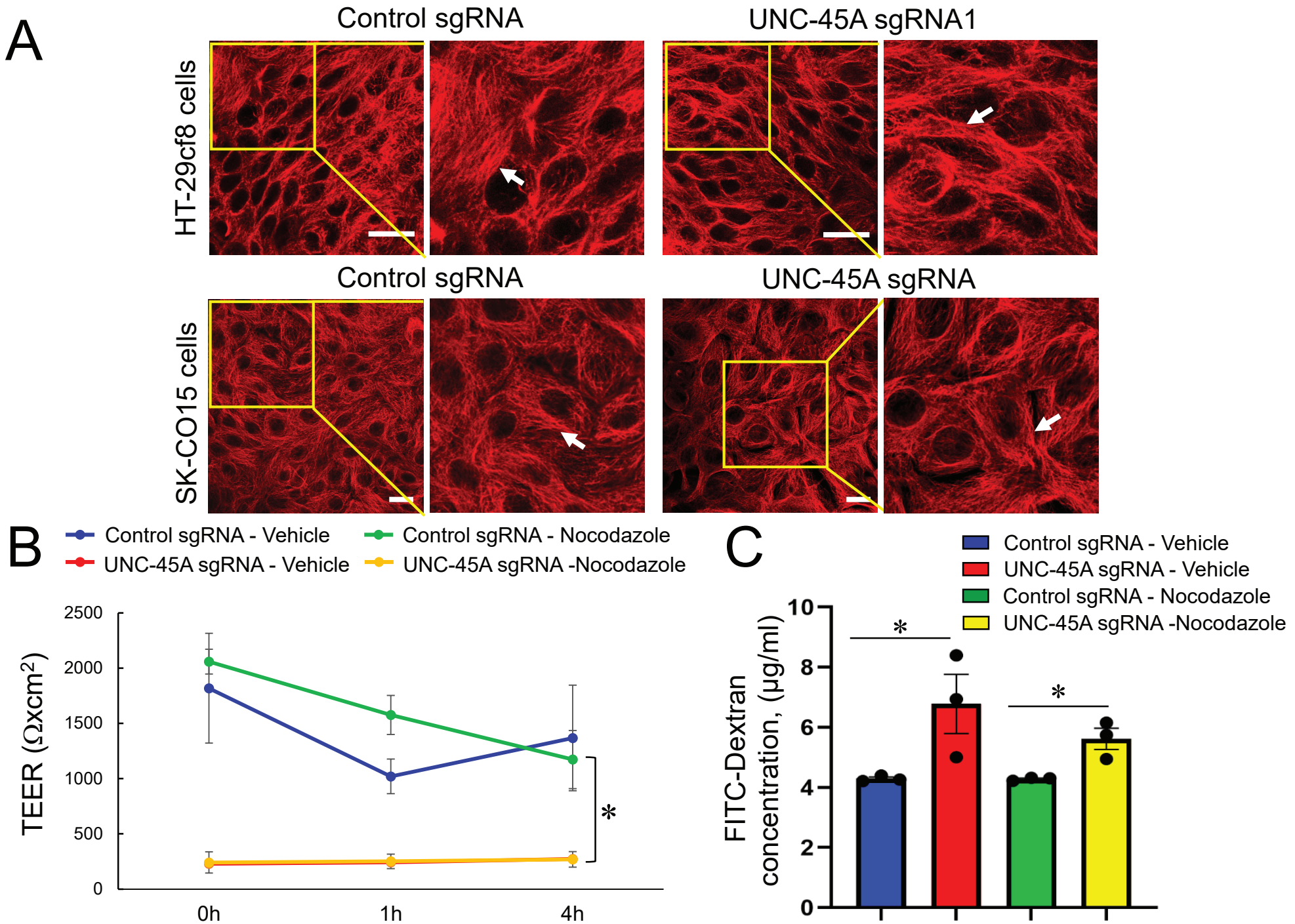

Figure S5. UNC-45A-dependent regulation of epithelial barrier does not depend on microtubules. (A) Confocal microscopy images of control and UNC-45A knockout HT-29cf8 and SK-CO15 cells immunolabeled for alpha-tubulin. Arrows point on normal organization of the apical microtubule network in control and UNC-45A knockout cells. Scale bar, 20 µm. (B,C) Transepithelial electrical resistance (TEER) of control and UNC-45A-depleted SK-CO15 cell monolayers treated for indicated times with nocodazole (30 µM). Means ± SE (n=3); *P< 0.05. Scale bars, 20 µm.

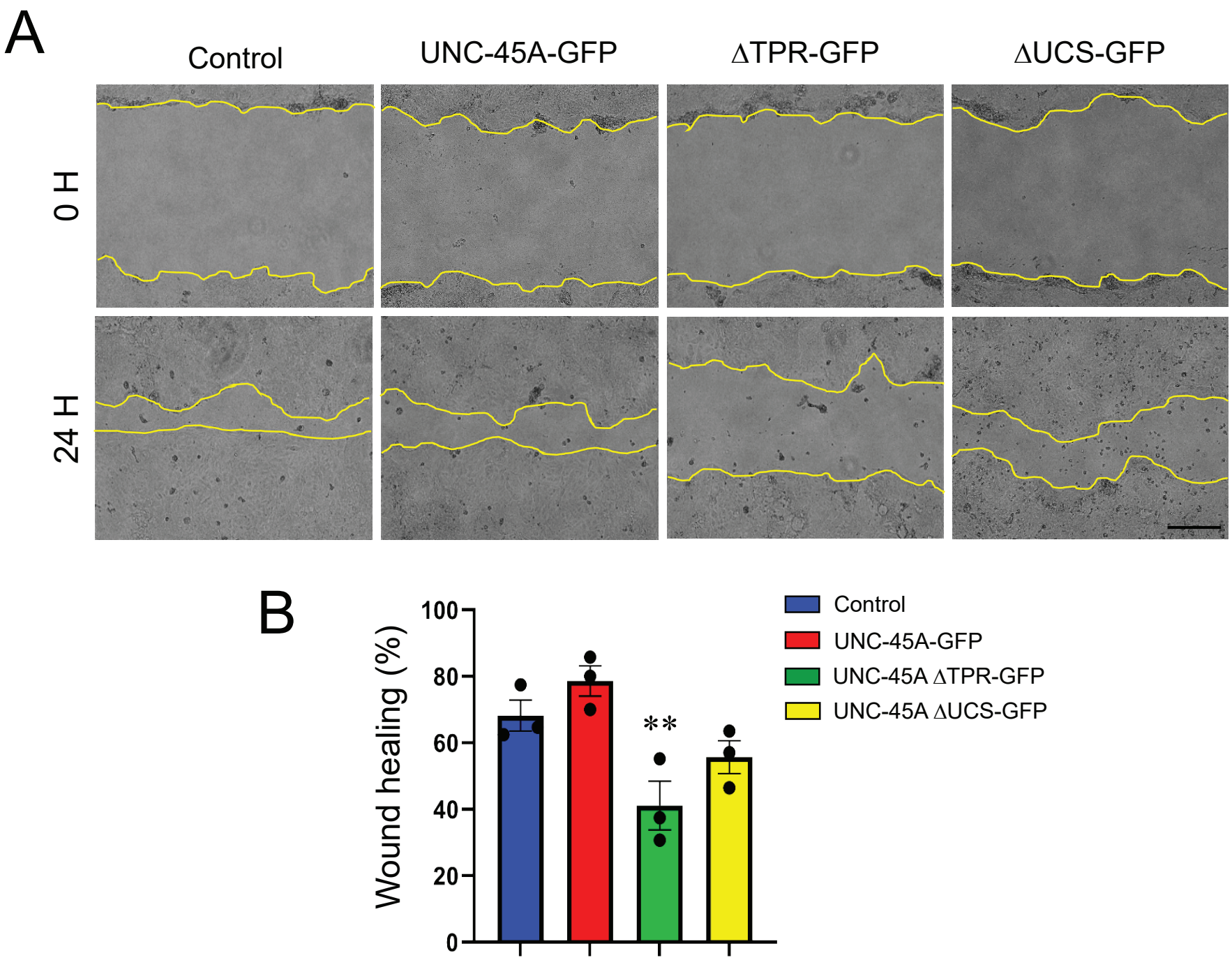

Figure S6. NM-II-interacting deletion mutant of UNC-45A selectively attenuates wound healing in IEC monolayers. (A,B) Wound healing of control SK-CO15 cell monolayers and cells expressing either GFP-tagged full-length UNC-45A or two different deletion mutants, ΔTPR-GFP (N-terminal truncated), or ΔUCS-GFP (C-terminally truncated). Representative wound images (A) and quantification of wound healing (B) are shown. Means ± SE (n=3); **P< 0.005. Scale bars, 200 μm. Data are representative of three independent experiments.

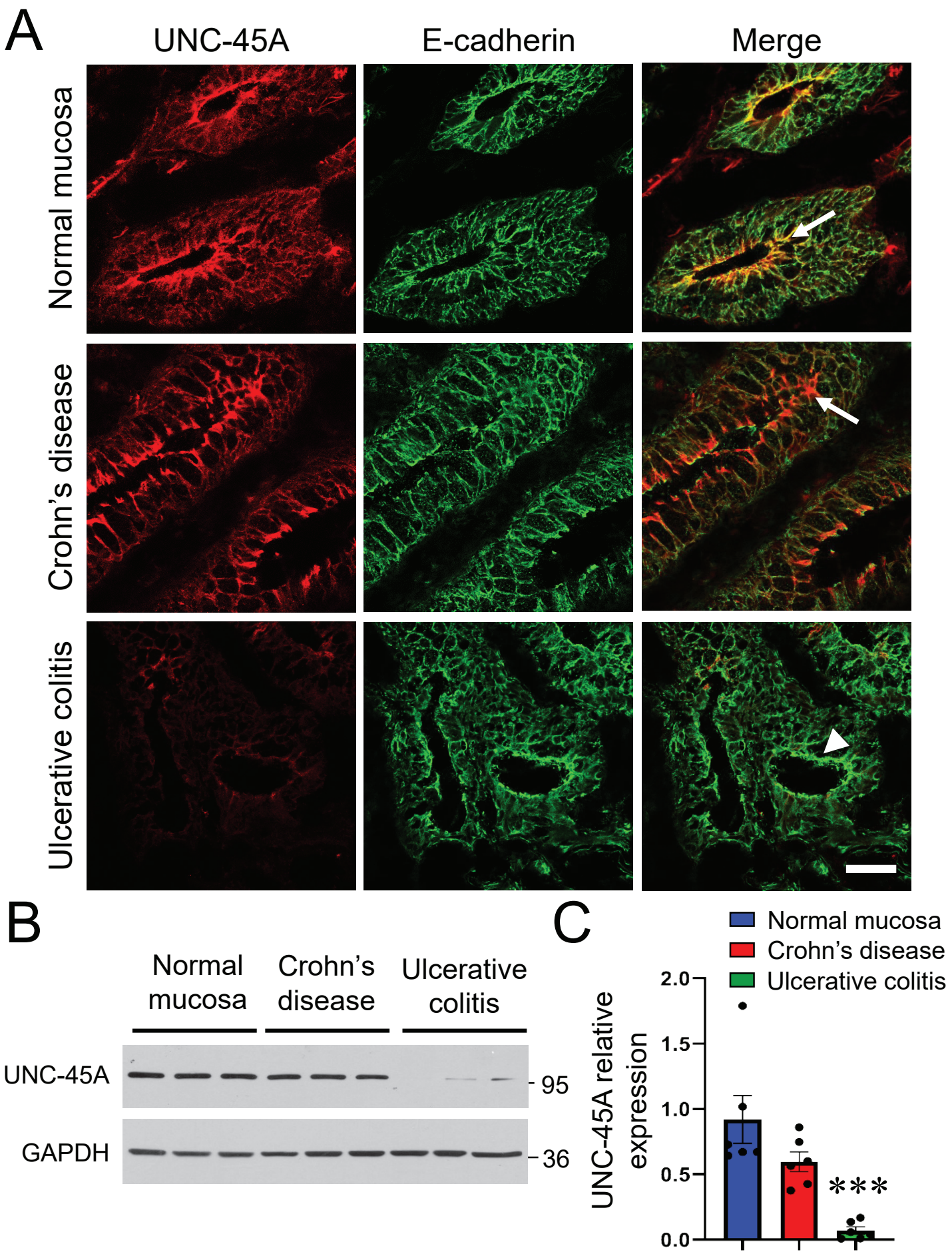

Figure S7. UNC-45A expression is down-regulated in the human colonic epithelium of patients with ulcerative colitis. (A) Dual-immunofluorescence labeling of UNC-45A (red) and E-cadherin (green) in whole thickness sections of normal colonic mucosa and colonic tissue of a Crohn's disease or ulcerative colitis patient. Arrows indicate UNC-45A enrichment at apical junctions in normal non-IBD mucosa and IEC of Crohn's disease patient and arrowheads show the loss of UNC-45A in IEC of ulcerative colitis patients. Images are representative of 6 patients per group. (B,C) Immunoblotting of UNC-45A expression in isolated human colonic epithelium of patients with Crohn's disease, ulcerative colitis and non-IBD controls. Representative immunoblots (B) and densitometric quantification (C) of UNC-45A expression are shown. Means ± SE (n=6); ***P<0.0005. Scale bar, 20 μm.